

A Risk Prediction and Clinical Guidance System for Evaluating Patients with Recurrent Infections.

Authors:

^{1,2,3}Nicholas L. Rider, DO*; ^{1,2}Gina Cahill, MPH; ^{1,4†}Tina Motazed, MD; ³Lei Wei, MS; ³Ashok Kurian; ^{1,2}Lenora M. Noroski, MD, MPH; ^{1,2}Filiz O. Seeborg, MD, MPH; ^{1,2}Ivan K. Chinn, MD; ⁶Kirk Roberts, PhD

¹Baylor College of Medicine, Houston, TX (USA)

²Section of Immunology, Allergy and Retrovirology, Texas Children's Hospital, Houston, TX (USA)

³Department of Information Services, Texas Children's Hospital, Houston, TX (USA)

⁴Massachusetts General Hospital, Boston, MA (USA)

⁵The University of Texas School of Biomedical Informatics, Houston, TX (USA)

*Denotes primary and corresponding author.

Nicholas L. Rider, D.O.

1102 Bates Street

Feigin Center, Suite 330

Texas Children's Hospital

Houston, TX 77030

nlrider@bcm.edu

† Dr. Motazed was a resident at Baylor College of Medicine during the majority of her contribution to this work. Presently she is a fellow in training at The Massachusetts General Hospital.

Keywords: Probabilistic Model, Bayesian Network, Machine Learning, Artificial Intelligence, Predictive Analytics, Prescriptive Analytics, Primary Immunodeficiency, Risk Assessment

Abstract:

Background:

Primary immunodeficiency diseases represent an expanding set of heterogeneous conditions which are difficult to recognize clinically. Diagnostic rates outside of the newborn period have not changed appreciably. This concern underscores a need for novel methods of disease detection.

Objective:

We built an artificial intelligence model to provide real-time risk assessment about primary immunodeficiency and to facilitate prescriptive analytics for initiating the most appropriate diagnostic work up. Our goal is to improve diagnostic rates for primary immunodeficiency and shorten time to diagnosis.

Methods:

We extracted data from the Texas Children's Hospital electronic health record on a large population of primary immunodeficiency patients (n = 1762) and age-matched set of controls (n = 1698). From the cohorts, clinically relevant prior probabilities were calculated enabling construction of a Bayesian network probabilistic model. Our model was constructed with clinical-immunology domain expertise, trained on a balanced cohort of 100 cases-controls and validated on an unseen balanced cohort of 150 cases-controls. Performance was measured by area under the receiver operator characteristic curve (AUROC).

Results:

Our Bayesian network was accurate in classifying immunodeficiency patients from controls (AUROC = 0.945; $p < 0.0001$) at a risk threshold of $\geq 6\%$. Additionally, the model was 89% accurate for categorizing validation cohort members into appropriate International Union of Immunological Societies diagnostic categories.

Conclusion:

Artificial intelligence methods can classify risk for primary immunodeficiency and guide management. Our Bayesian network enables highly accurate, objective decision making about risk and guides the user towards the appropriate diagnostic evaluation for patients with recurrent infections.

Introduction:

Infectious diseases contribute substantially to the costs of healthcare. For invasive *Streptococcus pneumoniae* alone, one estimate suggests that \$3.5 billion US Dollars (USD) are spent in direct costs for complications related to this single organism.[1] Among individuals who suffer infectious disease, a subsection will have ongoing risk of morbidity and mortality owing to an underlying genetic susceptibility. Such patients with primary immune defects (PI) often present in subtle fashion and may be mistaken for individuals with routine infection leading to diagnostic delay and death.[2]

Once thought to be rare, there are now 416 distinct PI diseases with 430 molecular etiologies known.[3] However, due to improved understanding about its biology and expanded testing capabilities, PI is now estimated to affect between 1:1000 to 1:5000 individuals and our prior work suggest that upwards of 1% of the general population may have features of PI risk.[4-6] Yet, early recognition of PI remains a challenge with time to diagnosis remaining largely fixed over the past 4 decades and is estimated at 7.5 – 9 years from symptom onset.[2] Projected annual costs for PI patients prior to diagnosis is nearly \$140,000 USD which may be reduced by approximately \$78,000 USD following diagnosis.[7, 8] In order to spare costs and undue morbidity, efforts are underway to facilitate early PI diagnosis and treat affected patients in a precise manner.[4, 9]

To aid in disease diagnosis, artificial intelligence methods can assist in population-wide and individual-level risk assessment.[10, 11] In particular, models which meld reasoning and uncertainty can facilitate diagnosis amongst at-risk individuals.[12] Bayesian networks (BNs) are one such model which combine relevant features, joint probability distributions and an

intuitive structure to answer questions in biomedicine.[13] Specifically, BNs have proven useful for clinical decision support for detecting lung cancers, prediction of heart failure, computing survival for individuals with colon cancer, aiding in liver disease evaluation and enabling pathology specimen evaluation among other use cases.[6, 14-19] It is for these reasons that we chose to build a BN for PI risk prediction and clinical guidance.

More specifically, BNs are probabilistic graphical models which embed data, expert opinion or a combination of the two into an intuitive graph thereby enabling reasoning given inherent uncertainty.[20] The basic structure of a BN (Fig. 1A) consists of nodes, each representing a variable, and arcs (arrows) which connect nodes in a causal relationship.[21] Underlying this intuitive and transparent structure are Bayes' theorem and Bayesian statistics which allow for calculating conditional and joint probability distributions across many variables within the network.[22, 23] The BN allows for both data and domain knowledge to be packaged into a single model that can yield insights about real-world probabilities, can be updated with new data or opinion over time and can tolerate missing information.[13, 20, 21] Here, we describe a BN which both assesses risk of underlying primary immunodeficiency and provides clinical guidance. (Fig. 1B) Our network model was constructed by an expert immunologist but the parameters (i.e. conditional probabilities) were learned entirely from data. Our model may be embedded within an electronic health record (EHR) via app-program interface (API) for the purposes of analyzing large-scale data in real time; alternatively, it may be clinician facing for data entry at the point of care to assess a given patient's risk and guide diagnosis

Results:

PI Cohort vs. Control Cohort:

Demographic statistics for the PI and control populations are shown in Table 1. The proxy for social determinants of health (SDOH) and healthcare access via assessment of insurance coverage and type was similar between groups (PI Cohort -52% Private, 45% Public, 3% Unknown; Control Cohort-48% Private, 50% Public, 2% Unknown). Network feature nodes are shown in Table 2 and were all significantly different in the PI vs. control cohorts (p-value <0.0001).

Risk Calculation (Cohort vs. Controls):

Performance of the BN on our validation cohort is shown in Figure 3. Individual risk calculation is displayed for the immunodeficient and control patients (Fig. 3A) as a single assessment for a given patient at the time of chart review. Classification performance is shown in Figure 3B and displayed as a receiver operator characteristic curve (ROC). The ROC analysis predicted best model performance at a risk cutoff of >5.5% (Sensitivity = 87%; CI(77%-93%) and Specificity = 91%; CI(82%-96%)). The corresponding BN performance measures were subsequently calculated as reported in Table 3 for risk calculation >5.5%.

Prescriptive Output – Directing Clinical Management:

Individuals within the PI validation cohort (n = 75) had 20 distinct PI disorders spanning the first 8 IUIS category tables. (Fig. 4A) Within the validation cohort, most had a Table 1/Table 2 (T/CID) related disorder (n = 32; 43%) or a Table 3 (PAD) related disorder (n = 26; 35%). Of

the remaining disease categories, Table 4 (PIRD) comprised 1%(n = 1), Table 5 (PD) comprised 8%(n = 6), Table 6 (ID) comprised 3%(n = 2), Table 7 (AID) comprised 4%(n = 3) and Table 8 (CD) comprised 1%(n = 1).

Model performance for predicting each patient's top 2 most likely IUIS disease categories is shown in Figure 4B. The BN was most successful in diagnosing patients with T/CID and phagocytic disorders. It was moderately effective in classifying antibody deficient patients appropriately. Additionally, the BN accurately classified patients with immune dysregulation, innate disease and autoinflammatory disease, but failed to classify the one complement disorder patient in our cohort. Overall BN model accuracy for determining patients across any studied IUIS category was 89%. It was 86% accurate if patients with table 1-3 disorders were omitted (n = 17).

Bayesian Network Functionality & Usability:

Data flow through the BN occurs once patient information is instantiated by an end-user (via our web portal for example - <https://bcm-demo.bayesfusion.com/dashboard.html?id=3gml3vd510t3qhb366xg3uevp>) or by analyzing diagnostic codes by EHR automatic feed via an API.(Supplemental Fig. 1B & C) The native structure is shown in Panel A; however, one can see the outputs for "Risk" and IUIS Category change depending upon data input. As displayed in Supplemental Figure 1B.1 & 1B.2 a patient's data with X-linked agammaglobulinemia (XLA) and associated clinical features are instantiated. The BN then provides an updated risk prediction and a prescription about the most likely diagnostic category (i.e. PAD) which can then inform the initial immunological workup. Supplemental Figure 1C.1 &

1C.2 shows information flow for a patient with chronic granulomatous disease (CGD) whose clinical findings are instantiated. Here risk is again updated from baseline and the prescriptive component selected PD as the top predicted IUIS category. A schematic of the proposed workflow is shown in Figure 5.

Discussion:

Knowledge about the biology of PI is expanding rapidly; however, overall diagnostic rates have not appreciably improved.[2, 3, 5] Therefore, novel disease-detection methods are needed such as digitizing relevant phenotypes and leveraging health information technology functionality. Here we demonstrate that concepts related to PI can be learned from readily-available, EHR-mined, structured data and embedded within a transparent (Fig. 1B) machine learning model that accurately provides both risk assessment and clinical guidance(i.e. ICDCs; Table 2, Figure 2). The model, a BN, allows for concept linking driven by domain expertise thereby enabling information flow in a rational manner for disease detection.[6, 14, 24, 25] This model can be deployed in almost any clinical setting and may learn over time as population specific conditional probabilities are accumulated with ongoing accuracy refinement.[26, 27]

Our model performed well on an unseen validation cohort of 75 patients with PI possessing a diverse range of diseases across the IUIS spectrum. (Table 3, Figure 3 & Figure 4) The AUROC (0.945; $p < 0.0001$, Figure 3B) suggests robust model classification of PI patients vs. control individuals. Training of the model consisted of analyzing 50 PI patients and 50 controls to assess performance which allowed us to identify gaps in concept relationships (Figure 2). Figure 3A shows considerable scatter across risk scores for the PI validation cohort; however,

the mean group score was significantly different from that of the controls (53.1 ± 38.1 vs. 6.9 ± 20 ; $p < 0.000001$) providing evidence that our model's inference about PI is sound. Importantly, our age-matched and SDOH-similar control group consisted of patients with varying medical complexity themselves but not PI. Diagnoses among this group included cystic fibrosis, trisomy 21, acute lymphoblastic leukemia, solid organ cancers, asthma, complex congenital heart disease and complex genetic disease. Therefore, accurately distinguishing PI from our controls is likely a more challenging task than classification against the general pediatric population. We take this as evidence of real-world model fitness and utility for our BN.

In addition to risk prediction, our model provides a prescriptive outcome to facilitate appropriate diagnostic evaluations and initiate referral if needed (Figure 4 & Figure 5). The BN's ability to direct a diagnostic approach is two-fold (Figure 5). First, a clinician's threshold for testing should be triggered by their clinical impression and a risk score $\geq 6\%$. The next question, "what do I do now?", can be answered via guidance about the most likely IUIS category. Given noted phenotypic heterogeneity among PI disorders, we assumed the initial predicted IUIS category would not be sufficiently inclusive; thus, we built our BN to predict the top 2 IUIS categories for each PI patient.[28] Using this strategy, our model was able to accurately define this class 89% of the time for the PI validation cohort (Figure 4). In 3 cases, the BN was unable to provide clinical guidance owing to lack of sufficient information. This scenario results in an equal probability prediction across IUIS categories and underscores the diagnostic uncertainty when scant patient information is available.

The prescriptive output of our model has utility for the primary care provider and clinical immunologist. Our expectation is that the provided decision guidance will inform clinical encounters by expediting appropriate testing and accurate diagnosis, assuming availability of recommended immune-diagnostic testing.[29] For the generalist or clinicians who are not generally focused on PI patients, we envision enabling early initial testing and referral to improve diagnostic rates. For the expert clinical immunologist, having relevant results in hand at the time of initial encounter should facilitate early implementation of best treatment practices and drive optimal outcomes for patients.

From an epidemiologic standpoint, our BN's best predicted risk score cutoff of $\geq 6\%$ is interesting in that it aligns well with our previous work in calculating a risk vital sign for PI.[4] There, analyzing a different population, we found 1% of the general population to be at medium-high risk for PI and subsequently $\sim 5\%$ of this group had PI or a concerning infectious diagnosis in the following year.[4] These results suggest that the prior probability of disease (prevalence) approaches 5% for individuals deemed to be of medium-high risk. Thus, all healthcare providers may expect approximately 1% of their patients to be at risk for PI. These individuals must then be distinguished from individuals with actual disease further reinforcing the importance of considering this vulnerable patient population amongst anyone with infections.

Here, we hypothesize that informatic methods may inform the diagnostic process by combining disease-specific features and epidemiologic data to enable diagnosis. Such models require computational transparency, good performance and should extend optimal digital health workflows to align with clinical decision support (CDS) best practices.[30] Predictive

analytics allows for discrimination about what might happen in a given clinical scenario; whereas, prescriptive analytics focuses on what one should do about the prediction.[31] This BN packages these attributes and presents a dual output for each patient to the user. Given reported concerns about time pressure for healthcare providers, delays in diagnosis, increased costs and poor outcomes we hoped to address these obstacles with our model en route to lowering the bar for PI diagnosis.[2, 7, 32] Lastly, we wish to underscore that our view of AI's role in healthcare is that it should be rigorously validated but dutifully implemented to augment clinical decision making and extend clinical efforts for making use of big data in a way that serves the patient and provider.[33, 34] With this perspective AI/machine learning aids the clinician and makes health information technology more useful.

Limitations & Future Directions:

While our model performed very well with the validation cohort, we need to test it prospectively on larger numbers of patients. Also, it will be helpful to have a larger number of end-users provide feedback about our web-interface usability. Future work in this regard will focus on expanded testing and soliciting expert immunologist opinions broadly as they use the BN for patient assessments.

Another limitation of our study was the somewhat biased PI cohort with a large number of 22q11.2 deletion syndrome patients ($n = 24$). The model was very accurate in predicting their IUIS class, but some of these individuals may have been detected via TREC-based newborn screening. This bias is reflected in our overall PI population which contained many DiGeorge Syndrome patients cared for at our center. Additionally, we had limited representation of

patients with disorders falling into the IUIS Tables 4, 6, 7 and 8. Patients with these disorders are less prevalent among PI as a whole; however, such information could be mined from registries or pooled from other centers and used to improve model fitness. Also, we decided to exclude inference about marrow failure syndrome and PI phenocopies (IUIS Tables 9 & 10) here; thus, patients with these disorders might not be detected with the current version of our network. We can track model performance prospectively about patients with such disorders and easily modify the network as needed.

Lastly, we plan to investigate additional variables that can be added to further improve network performance. Our BN performs very well in validation with only 36 nodes; however, it is likely that additional informative features will drive further improvement.

Conclusions:

Machine learning may facilitate diagnosis of patients with PI. Combining domain expertise and readily available EHR structured data with well-defined machine learning models provides an effective tool for risk assessment of PI.

Methods:

Ethics Statement:

This study was approved by the Baylor College of Medicine Institutional Review Board (H-38501). All patient data remained confidential and was retained in the Texas Children's Hospital system.

Cohort Analysis:

Patients from Texas Children's Hospital (TCH) with immunodeficiency were identified by having at least 2 ICD10 codes (ICDCs) entered at different time points (2008 – 2018) which was consistent with a primary immunodeficiency as categorized by the American Academy of Asthma, Allergy and Immunology (AAAAI); <https://www.aaaai.org/Aaaai/media/MediaLibrary/PDF%20Documents/Practice%20Management/finances-coding/ICD-10-Codes-Immunodeficiencies.pdf>). The PI cohort was comprised of 1762 individuals. (Table 1) In contrast, control data were specified by an age matched set of patients from TCH who did not harbor one of the PI codes and consisted of 1698 individuals. This was termed the "Control Cohort". For each cohort, all ICDCs over 24 months were extracted from the TCH EHR (Epic Clarity Database). Individual, unique ICDCs were compiled for each cohort, counted, normalized and assessed for differences between groups. Relevant ICDCs were defined as having a significantly increased frequency among PI patients and associated relevance to PI based upon domain expertise. Features for construction of the BN

were derived from relevant ICDCs with pertinence to human immunological disease as determined by an expert clinical immunologist (NLR). (Supplemental Figure 1)

Prior Probability Calculations:

We calculated prior probabilities for 36 different feature nodes for both PI the and Control populations. Each feature had corresponding ICDCs as listed in Table 2 and was representative of the node concept.[35] Prior probabilities were calculated by taking the total number of occurrences for each ICDC of interest and dividing by the total number of patients in that specific cohort (either PI or Control). These conditional probabilities (i.e. fraction of individuals with the condition given PI or given non-PI) were then used to create the Bayesian Network as described below. When there were no occurrences of a given clinical entity among controls, we arbitrarily set the conditional probability to be 0.0001% since a prior value of “0%” or “100%” does not accurately reflect real-world uncertainty. Learning prior probabilities for the “meningococcal disease” node general risk differed from the rest in that it was derived from literature rather than from data; additionally, data about patients receiving complement inhibitor therapy were used as a surrogate for meningococcal disease risk in PI.[36, 37]

Bayesian Network Construction:

Network structure was designed to facilitate clinical decision making derived from information obtained from a thorough history, physical examination and complete blood count (CBC/differential) without need for advanced immunological testing. The BN described was constructed using GeNIe Modeler available free of charge for academic research and teaching use from BayesFusion, LLC (<http://www.baysefusion.com/>). Feature nodes were created and

added from learning as described above. In total 36 feature nodes were used (10 history/physical examination, 5 laboratory, 5 general infections, 16 highly informative infection/condition) which corresponded to 79 distinct ICDCs. (Figure 1B, Supplemental Fig 1, & Table 2) Contained within each node are the conditional probabilities of finding that variable in the PI cohort (“med-high risk”) and within a general pediatric population (“low risk”). We assumed the general population overall *risk* to be 1% for PI. This threshold was determined experimentally from our prior work where 2188 of 185,892 individuals (1.2%) were deemed at medium-high risk for PI.[4] Our network structure, dynamic information flow and intuitive dashboard can be found at <https://bcm-demo.bayesfusion.com/dashboard.html?id=3gml3vd510t3qhb366xg3uevp>

The BN structure was designed such that all 36 diagnostic variables/features are connected to the risk node. Risk is then calculated by employing Bayes’ Theorem for single or multiple conditions as features are instantiated for a given patient. Feature nodes were also connected via arrows (edges) to each of 8 IUIS disorder categories described as: T-cell/Combined (T/CID), Predominantly Antibody(PAD), Immune Dysregulatory(PIRD), Phagocyte(PD), Innate(ID), Autoinflammatory(AID) and Complement(CD). We combined Tables 1 & 2 from the Expert Committee report into one category and did not include bone marrow failure syndromes or PI phenocopies. This resulted in 7 IUIS disorder network nodes. Node connections were created based upon their contribution to a phenotype for that category as expected by domain expertise or as described in Tangye et al.[3] (Supplemental Fig. 1) Arrow directions indicate dependency (e.g. moving in the direction of the arrow one can say “*this* is dependent upon *that*”). For a given patient, IUIS category likelihood ranking was calculated by

summing individual conditional probabilities among the present feature nodes. The output IUIS categories with the highest “yes” probability suggest the most appropriate starting point in the diagnostic workup for an individual patient. The probability output shown is compared to the general population; therefore, magnitude change from baseline is more important than the absolute percentage shown.

Bayesian Network Training & Validation:

From our immunodeficient and control cohorts, 250 patients (125 disease, 125 control) were randomly selected to train and validate the network. For the training and validation cohorts, each patient’s clinical and relevant laboratory history was confirmed by medical record chart review. Additionally, we assessed SDOH via analysis of insurance type as a proxy to normalize for health care access across the cohorts. Features were determined and entered into the BN for calculation of risk and IUIS category ranking. (Figure 2) For PI cohort training and validation, we excluded patients with a diagnosis of severe combined immunodeficiency (SCID) since they should have been detected asymptotically via newborn screening. Similarly, patients with secondary immunodeficiency were excluded from the PI group but not from the control group.

After initial model build(i.e. node selection, probability embedding and arc-setting), we trained our BN with 50 PI patients and 50 controls(“*training data*”; Fig. 2). This allowed for tuning of the BN, adding additional relevant features and provided insights about node connections. Once the network was restructured, we performed validation testing with 75 previously unseen patients from each cohort(“*validation data*”; Fig. 2) Members of the

validation cohorts had similar ages (mean control age = 8 ± 5 yrs; mean PI age = 8 ± 3 years).

Network performance was assessed by receiver operator characteristic (ROC) curve analysis on the validation cohort.

Statistical Methods:

Descriptive statistics for the PI and control cohorts were determined using Microsoft Excel and are shown in Table 1. Significance testing and the ROC curve analyses were conducted in Prism GraphPad version 8 (<https://www.graphpad.com>).

Data Availability Statement:

Patient protected health information (PHI) is not available; however, all clinical data used to generate inference by the Bayesian network is available. Most relevant data from our study are included in the supplementary materials. Additional data availability may be made available from the corresponding author on reasonable request.

Acknowledgements:

We wish to thank the Jeffrey Modell Foundation for grant funding (JMF Translational Grant-58293-I). We are also grateful to our colleagues who contributed clinical care to patients whose data was analyzed here. We acknowledge Tomasz Sowinski of BayesFusion (<https://www.bayesfusion.com/>) for access to the Bayesian network modeling tool made freely available to academicians and Mr. Sowinski's substantial work with creating the web-based dashboards.

Author Contributions: NLR conceived the study, wrote the manuscript, had access to all data, oversaw data analysis, prepared the manuscript and helped design the web dashboard. GC performed statistical analyses and contributed to manuscript construction and review. TM, LW, AK, LMN, FOS and IKC extracted and contributed data and provided critical review of the manuscript. KR provided critical review of the network methods, contributed to the study concept design and manuscript review.

Competing Interest Statement: GC, TM, LW, AK, LMN, FOS, IKC and KR have nothing to disclose. NLR received consulting fees for scientific advisory activities with Takeda Pharmaceuticals, Horizon Therapeutics and CSL Behring. He also receives royalties from Wolters Kluwer for topic contribution to UpToDate.

Funding: This work was funded through a Translational Research Grant (Award No - 58293-I) by the Jeffrey Modell Foundation

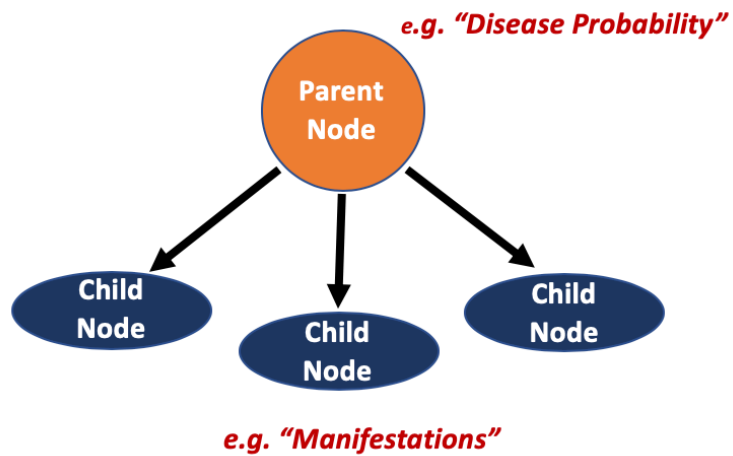
Bibliography:

- [1] S. S. Huang *et al.*, "Healthcare utilization and cost of pneumococcal disease in the United States," *Vaccine*, vol. 29, no. 18, pp. 3398-412, Apr 18 2011.
- [2] I. Odnoletkova *et al.*, "The burden of common variable immunodeficiency disorders: a retrospective analysis of the European Society for Immunodeficiency (ESID) registry data," *Orphanet J Rare Dis*, vol. 13, no. 1, p. 201, Nov 12 2018.
- [3] S. G. Tangye *et al.*, "Human Inborn Errors of Immunity: 2019 Update on the Classification from the International Union of Immunological Societies Expert Committee," *J Clin Immunol*, Jan 17 2020.
- [4] N. L. Rider *et al.*, "Calculation of a Primary Immunodeficiency "Risk Vital Sign" via Population-Wide Analysis of Claims Data to Aid in Clinical Decision Support," *Front Pediatr*, vol. 7, p. 70, 2019.
- [5] Q. Zhang, P. Frange, S. Blanche, and J. L. Casanova, "Pathogenesis of infections in HIV-infected individuals: insights from primary immunodeficiencies," *Curr Opin Immunol*, vol. 48, pp. 122-133, Oct 2017.
- [6] A. Stojadinovic *et al.*, "Clinical decision support and individualized prediction of survival in colon cancer: bayesian belief network model," *Ann Surg Oncol*, vol. 20, no. 1, pp. 161-74, Jan 2013.
- [7] V. Modell *et al.*, "Global study of primary immunodeficiency diseases (PI)--diagnosis, treatment, and economic impact: an updated report from the Jeffrey Modell Foundation," *Immunol Res*, vol. 51, no. 1, pp. 61-70, Oct 2011.
- [8] B. Sadeghi, H. Abolhassani, A. Naseri, N. Rezaei, and A. Aghamohammadi, "Economic burden of common variable immunodeficiency: annual cost of disease," *Expert Rev Clin Immunol*, vol. 11, no. 5, pp. 681-8, May 2015.
- [9] A. Kwan *et al.*, "Newborn screening for severe combined immunodeficiency in 11 screening programs in the United States," *JAMA*, vol. 312, no. 7, pp. 729-38, Aug 20 2014.
- [10] A. Esteva *et al.*, "A guide to deep learning in healthcare," *Nat Med*, vol. 25, no. 1, pp. 24-29, Jan 2019.
- [11] A. Hosny *et al.*, "Deep learning for lung cancer prognostication: A retrospective multi-cohort radiomics study," *PLoS Med*, vol. 15, no. 11, p. e1002711, Nov 2018.
- [12] P. J. Lucas, L. C. van der Gaag, and A. Abu-Hanna, "Bayesian networks in biomedicine and health-care," *Artif Intell Med*, vol. 30, no. 3, pp. 201-14, Mar 2004.
- [13] P. Arora, D. Boyne, J. J. Slater, A. Gupta, D. R. Brenner, and M. J. Druzdzel, "Bayesian Networks for Risk Prediction Using Real-World Data: A Tool for Precision Medicine," *Value Health*, vol. 22, no. 4, pp. 439-445, Apr 2019.
- [14] M. B. Sesen, A. E. Nicholson, R. Banares-Alcantara, T. Kadir, and M. Brady, "Bayesian networks for clinical decision support in lung cancer care," *PLoS One*, vol. 8, no. 12, p. e82349, 2013.

- [15] N. A. Loghmanpour, R. L. Kormos, M. K. Kanwar, J. J. Teuteberg, S. Murali, and J. F. Antaki, "A Bayesian Model to Predict Right Ventricular Failure Following Left Ventricular Assist Device Therapy," *JACC Heart Fail*, vol. 4, no. 9, pp. 711-21, Sep 2016.
- [16] A. C. Constantinou, N. Fenton, W. Marsh, and L. Radlinski, "From complex questionnaire and interviewing data to intelligent Bayesian network models for medical decision support," *Artif Intell Med*, vol. 67, pp. 75-93, Feb 2016.
- [17] H. Wasyluk, A. Onisko, and M. J. Druzdzel, "Support of diagnosis of liver disorders based on a causal Bayesian network model," *Med Sci Monit*, vol. 7 Suppl 1, pp. 327-32, May 2001.
- [18] D. E. Heckerman, E. J. Horvitz, and B. N. Nathwani, "Toward normative expert systems: Part I. The Pathfinder project," *Methods Inf Med*, vol. 31, no. 2, pp. 90-105, Jun 1992.
- [19] D. E. Heckerman and B. N. Nathwani, "Toward normative expert systems: Part II. Probability-based representations for efficient knowledge acquisition and inference," *Methods Inf Med*, vol. 31, no. 2, pp. 106-16, Jun 1992.
- [20] K. Korb and A. Nicholson, *Bayesian Artificial Intelligence*, 2nd ed. Boca Raton, FL: CRC Press, 2011, p. 452.
- [21] D. E. Heckerman, "A Tutorial on Learning With Bayesian Networks," Microsoft Corporation 1995, Available: <http://tomlr.free.fr/Math%E9matiques/Fichiers%20Claude/Auteurs/Aprov070125/Heckerman%20-%20A%20Tutorial%20On%20Learning%20Bayesian%20Networks.pdf>.
- [22] D. E. Heckerman and J. S. Breese, "Causal Independence for Probability Assessment and Inference Using Bayesian Networks," *IEEE Trans on Syst., Man and Cybernetics*, vol. 26, pp. 826-31, 1996.
- [23] M. Li, M. Hong, and R. Zhang, "Improved Bayesian Network-Based Risk Model and Its Application in Disaster Risk Assessment," *Int. J. Disast. Risk Sci.*, vol. 9, pp. 237-248, 2018.
- [24] A. Onisko and M. J. Druzdzel, "Impact of precision of Bayesian network parameters on accuracy of medical diagnostic systems," *Artif Intell Med*, vol. 57, no. 3, pp. 197-206, Mar 2013.
- [25] A. Onisko, M. J. Druzdzel, and R. M. Austin, "Application of Bayesian network modeling to pathology informatics," *Diagn Cytopathol*, vol. 47, no. 1, pp. 41-47, Jan 2019.
- [26] R. Daly, Q. Shen, and S. Aitken, "Learning Bayesian Networks: approaches and issues.," *The Knowledge Engineering Review*, vol. 26, no. 2, pp. 99-157., 2011.
- [27] H. Amirkhani, M. Rahmati, P. J. F. Lucas, and A. Hommersom, "Exploiting Experts' Knowledge for Structure Learning of Bayesian Networks," *IEEE Trans Pattern Anal Mach Intell*, vol. 39, no. 11, pp. 2154-2170, Nov 2017.
- [28] A. Stray-Pedersen *et al.*, "Primary immunodeficiency diseases: Genomic approaches delineate heterogeneous Mendelian disorders," *J Allergy Clin Immunol*, vol. 139, no. 1, pp. 232-245, Jan 2017.
- [29] F. A. Bonilla *et al.*, "Practice parameter for the diagnosis and management of primary immunodeficiency," *J Allergy Clin Immunol*, vol. 136, no. 5, pp. 1186-205 e1-78, Nov 2015.
- [30] J. E. Tchong *et al.*, "Optimizing Strategies for Clinical Decision Support," National Academy of Medicine, Washington, DC 2017.

- [31] M. S. Islam, M. M. Hasan, X. Wang, H. D. Germack, and E. A. M. Noor, "A Systematic Review on Healthcare Analytics: Application and Theoretical Perspective of Data Mining," *Healthcare (Basel)*, vol. 6, no. 2, May 23 2018.
- [32] E. Topol, *Deep Medicine: How Artificial Intelligence Can Make Healthcare Human Again*. New York, NY USA: Basic Books, 2019.
- [33] J. Wiens *et al.*, "Author Correction: Do no harm: a roadmap for responsible machine learning for health care," *Nat Med*, vol. 25, no. 10, p. 1627, Oct 2019.
- [34] M. Sendak *et al.*, "A Path for Translation of Machine Learning Products into Healthcare Delivery," *EMJ Innov.*, 2020.
- [35] B. T. Costa-Carvalho *et al.*, "Attending to warning signs of primary immunodeficiency diseases across the range of clinical practice," *J Clin Immunol*, vol. 34, no. 1, pp. 10-22, Jan 2014.
- [36] CDC. (2019, October 1). *Clinical Information: Meningococcal Disease: Technical and Clinical Information*. Available: <https://www.cdc.gov/meningococcal/clinical-info.html>
- [37] CDC. (2019, October 1). *Managing the Risk of Meningococcal Disease among Patients Who Receive Complement Inhibitor Therapy*. Available: <https://www.cdc.gov/meningococcal/clinical/eculizumab.html>

A.



B.

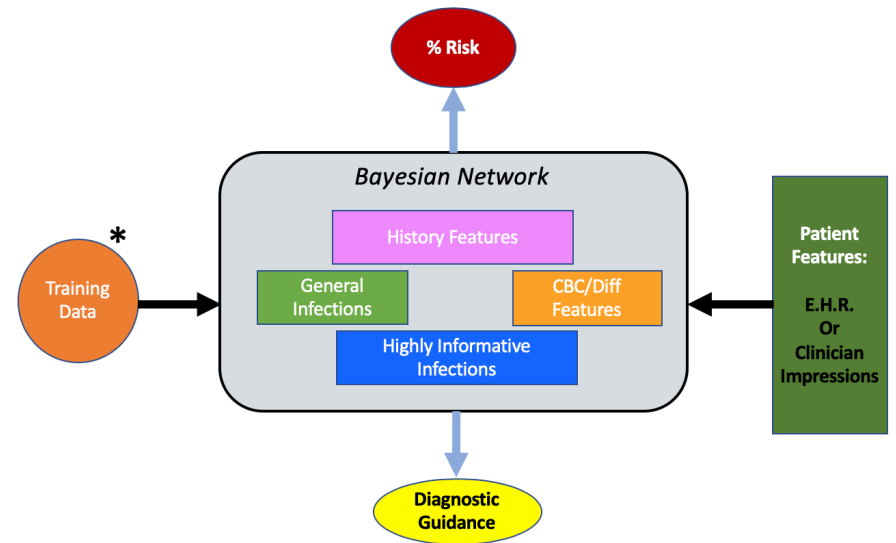


Fig. 1 Bayesian Network Structure. A. An example Bayesian network with parent and child nodes connected by arcs. B. The general structure of our network components. Training data(*may be updated over time) and patient features allow for improving inference (i.e. probabilities) and structure over time making these networks dynamic. (EHR = Electronic Health Record)

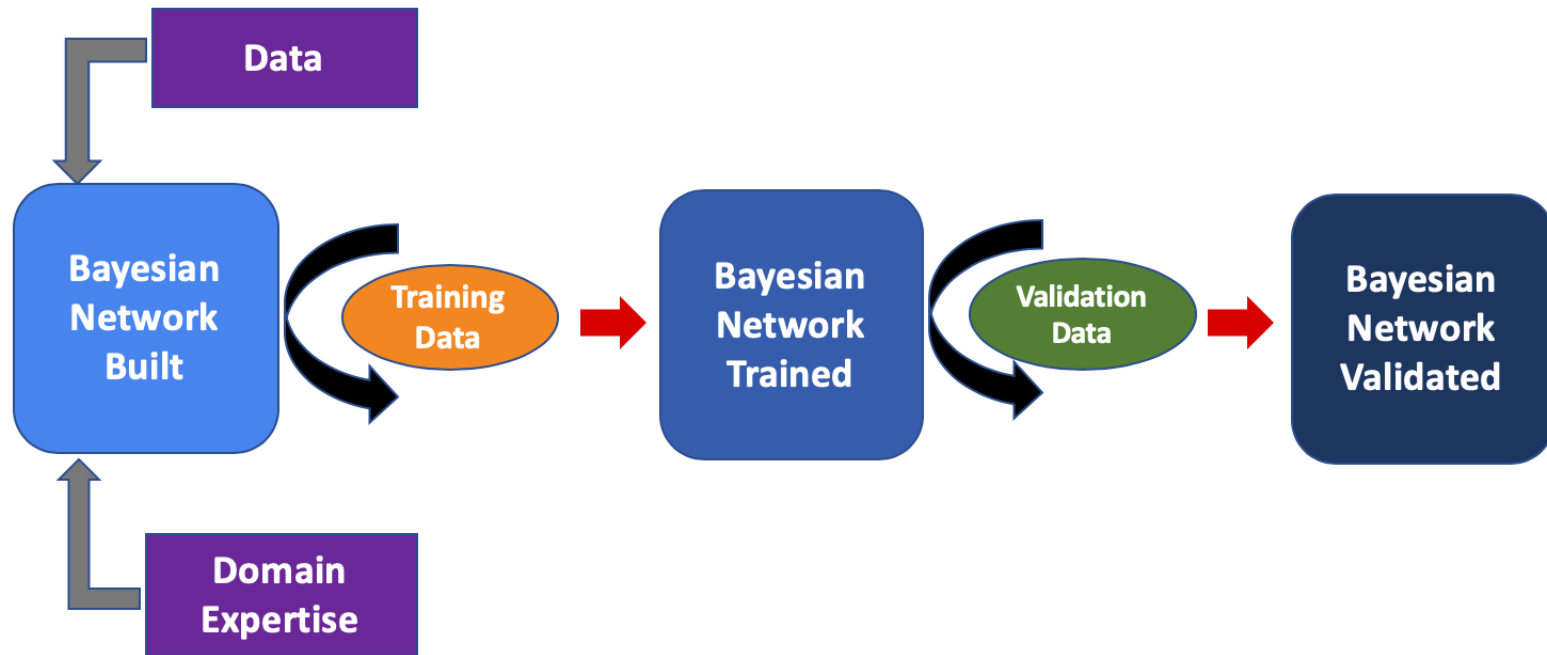


Fig. 2 Analytics Plan. Network construction, training and validation scheme. Here, 100 patients (50 PI and 50 Control) were used as training data and 150 (75 each cohort) were used as validation data.

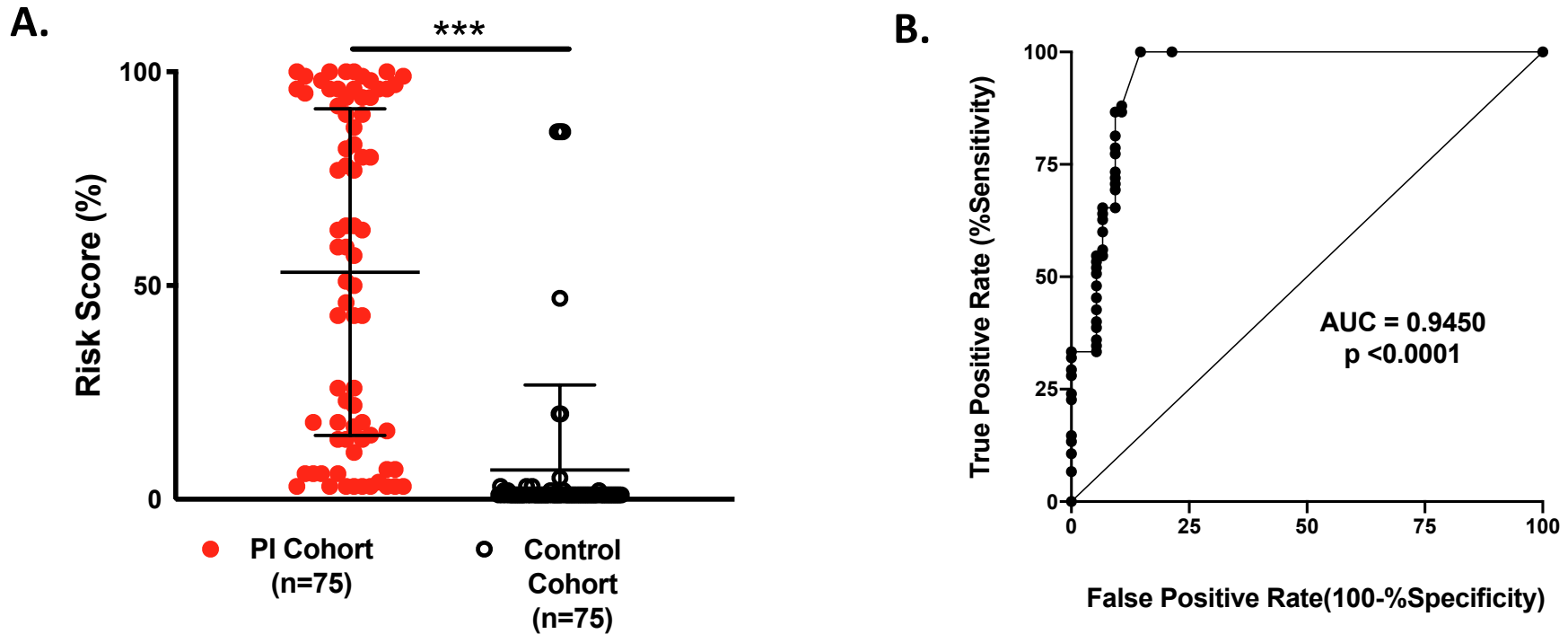


Fig.3 Network Validation. Validity testing of our BN for individual patients from the PI and Control cohorts. **A.** Mean risk scores between the two populations were significantly different (53% vs. 7%; $p < 0.000001$). **B.** Network performance as calculated by AUROC (Area under Receiver Operator Characteristic Curve) where an AUROC of 1.0 represents the ability of a model to discriminate between classes 100% of the time.

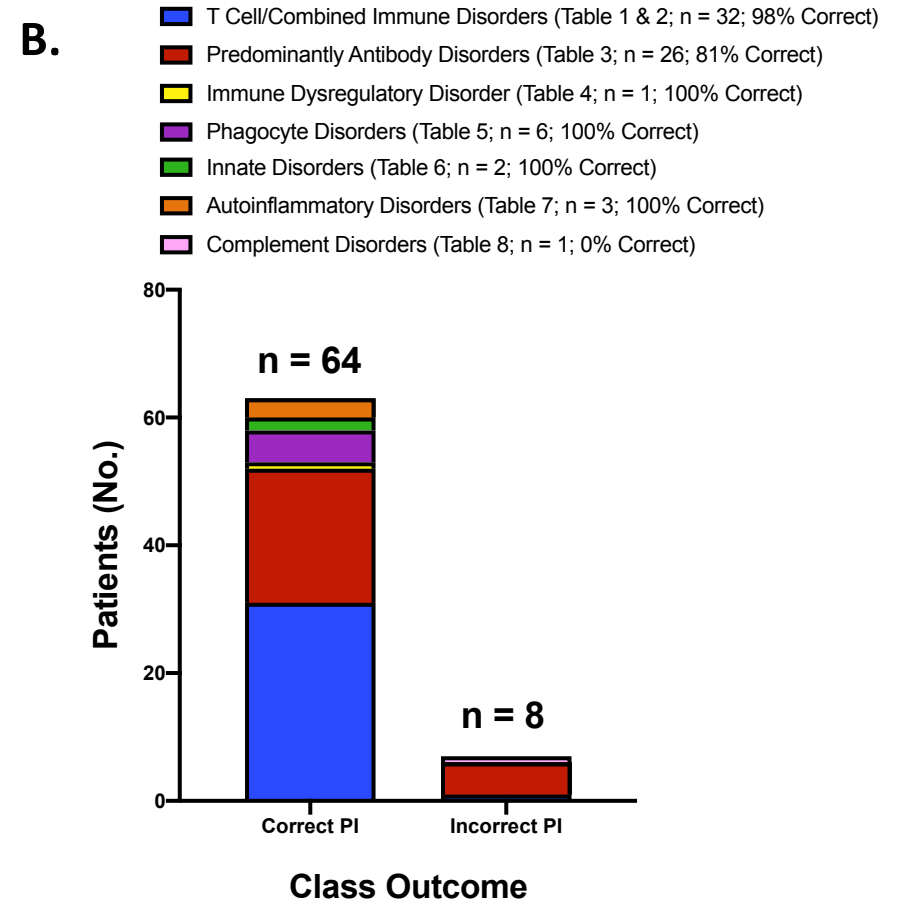
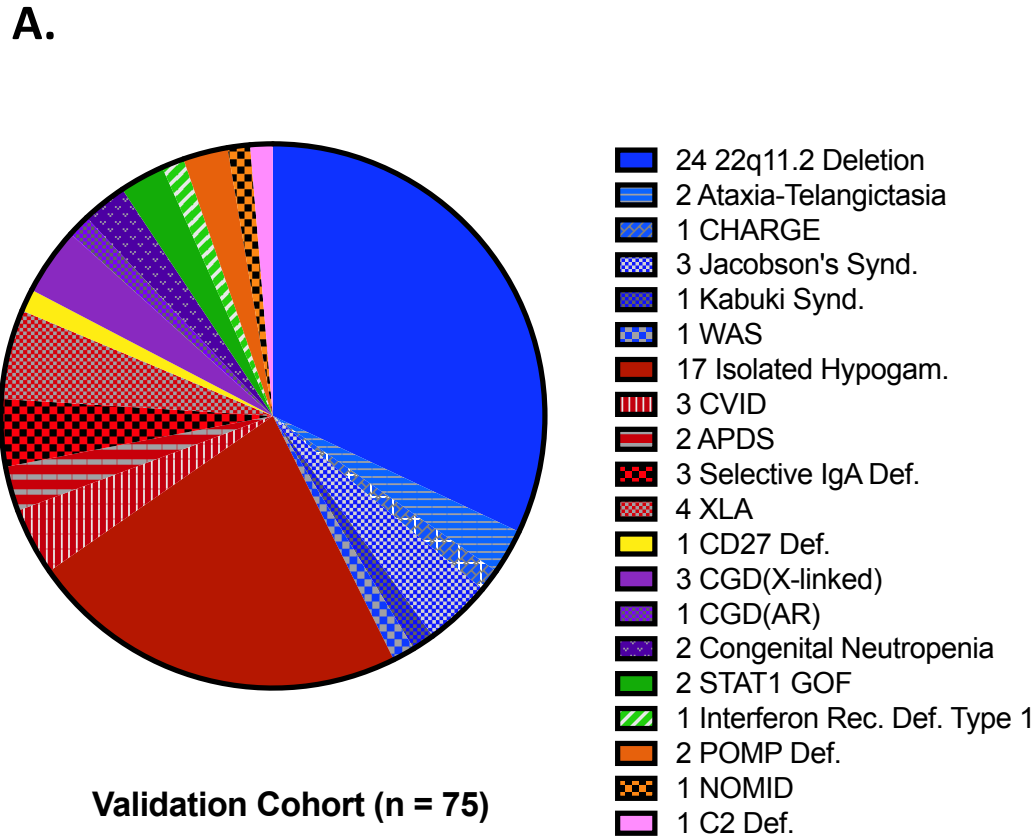


Fig. 4 Cohort Features & Network Outcomes. **A.** Validation cohort disorder spectrum. The IUIS groupings are clustered according to color (i.e. Blue=T/CID; Red=PAD; Yellow=PIRD; Purple=PD; Green=ID; Orange=AID and Pink=CD). **B.** BN performance for classifying each IUIS category and overall outcome. The legend displays category number and accuracy for our BN prediction. NOTE- 3 patients were not included here since insufficient input data were available and a class outcome could not be defined by the model. (Abbreviations: CHARGE-coloboma, heart disease, atresia of choanae, restricted growth, genital and ear abnormalities; WAS-Wiskott-Aldrich Syndrome; CVID-Common Variable Immunodeficiency; APDS-Activated Pi3K Delta Syndrome; XLA-X-linked Agammaglobulinemia; CGD-Chronic Granulomatous Disease; STAT1 GOF- Signal Transducer Activator of Transcription 1 Gain of Function; POMP-Proteasome Maturation Protein; NOMID-Neonatal Onset Multisystem Inflammatory Disease.)

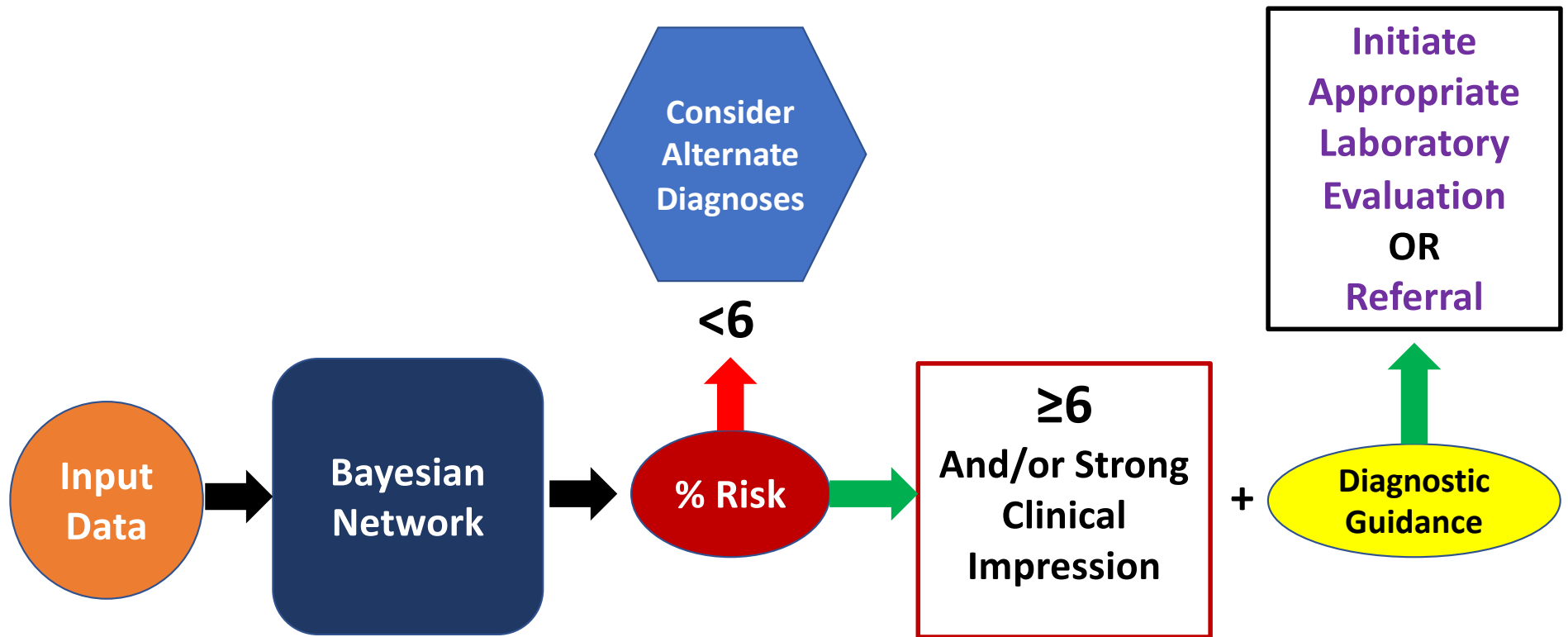


Fig. 5 Workflow Model. The proposed workflow for our model. Here, an end-user or EHR data feed can provide inputs via clinical impressions or diagnostic codes. The BN calculates a risk score which can subsequently be acted upon. It is important to note that it is the risk score and clinical impression should be taken together, which guide subsequent evaluation and management.

Table 1: Demographic Features of the Cohort

	PI Cohort (n = 1762)	Control Cohort (n = 1698)
Mean Age (yrs)	8 ± 4	7 ± 5
Sex		
Male	1001 (56.8%)	891 (52.5%)
Female	761 (43.2%)	807 (47.5%)
Ethnicity:		
Caucasian	793(45%)	552(33%)
Hispanic	606(35%)	601(35%)
Black	199(11%)	281(17%)
Asian	89(5%)	91(5%)
Unknown	75(4%)	173(10%)

Table 2. Network features with corresponding counts and conditional probabilities for each cohort.

Node Description (ICD Code(s))	Count PI Cohort(No.)	Conditional Probability PI Cohort (%)	Count Control Cohort (No.)	Conditional Probability Control Cohort (%)
Abscess (B43, G06, G07, J36, J85, K61, L02)	65	3.7	26	1.5
Aspergillus Infections (B44.0, B44.7, B44.9)	15	0.9	3	0.2
Ataxia(R27.0)	13	0.7	4	0.2
Auto-Immune Hemolytic Anemia (D59.1)	32	1.8	0	0.0001
Bronchiectasis (J47)	31	1.8	7	0.4
Dysmorphic Features (Q18.9, Q82.4, R62.52, Z36.4)	165	9.4	34	2.0
Encephalitis (A83, A84, A85, A86, G04)	10	0.6	2	0.1
Eosinophilia (D72.1)	35	2.0	0	0.0001
Failure to Thrive (R62)	473	26.9	194	11.4
Fatigue (R53)	171	9.7	50	2.9
Fibrosis (K74)	6	0.3	1	0.06
Granulomatous Skin Disease (L92)	41	2.3	14	0.8
Herpes Infections (A60, B00, B02, B10, B27)	100	5.7	15	0.9
Hypocalcemia (E83.51)	49	2.8	3	0.2
Iron Deficiency Anemia (D50.8)	63	3.6	13	0.8
Lymphadenopathy (R59.9)	64	3.6	38	2.2
Lymphoma (C81, C82, C83, C84, C85, C86, C88)	23	1.3	2	0.1
Lymphopenia (D72.810)	113	6.4	3	0.2
Meningococcal Disease (A39.xx)*	N/A	0.0001	N/A	1x10 ⁻⁷
Mycobacterial Disease (A31.9)	10	0.6	2	0.1
Neutropenia (D70)	246	14.0	18	1.1
Opportunistic Infections (A02, A31,B39, B55, B40, B59)	26	1.5	2	0.1
Organomegaly (R16)	50	2.80	8	0.5
Otorrhea, Chronic (H92.1)	91	5.2	39	2.3
Pneumonia (<2 episodes) (J13, J14, J15, J16, J17, J18)	134	7.6	66	3.9
Pneumonia (≥2 episodes) (J13, J14, J15, J16, J17, J18)	105	6.0	41	2.4
Polyarthritis (M00, M13)	13	0.7	1	0.06
Recurrent Fever (A68)	30	1.7	3	0.2
Sensorineural Hearing Loss (H90)	130	7.4	27	1.6
Sepsis (A40, A41, O85, P36)	104	5.9	9	0.5
Septic Shock (A41.9, R65.21)	95	5.4	9	0.5
Sinusitis (>4 episodes) (J01, J32)	89	5.1	23	1.4
Superficial Mycosis	16	0.9	1	0.06
Systemic Lupus Erythematosus	39	2.2	0	0.0001
Thrombocytopenia (D69.59, T45.IX5A)	75	4.3	7	0.4
Warts (B07)	7	0.4	4	0.2

* Denotes data learned from literature

Table 3: Network Performance (Risk Calculation)

	Score
Specificity	91%
Sensitivity	87%
PPV	91%
NPV	87%
Accuracy	89%
F1	88%

PPV-Positive Predictive Value; NPV-Negative Predictive Value; F1=F1 Score

Supplemental Table 1: Network Nodes and Associated ICD10 Code Information

Network Node Label	ICD10 Codes & Descriptions
Abscess	B43 - Chromomycosis and Pheomycotic abscess; G06 - Intracranial and Intraspinal abscess and granuloma; G07 - Intracranial and Intraspinal abscess and granuloma in diseases classified elsewhere; J36 - Peritonsillar abscess; J85 - Abscess of lung and mediastinum; K61 - Abscess of anal and rectal regions; L02 - Cutaneous abscess, furuncle, and carbuncle
Aspergillosis	B44.0 - invasive pulmonary aspergillosis; B44.7 - disseminated aspergillosis; B44.9 - aspergillosis, unspc
Ataxia	R27.0 - Ataxia, unspecified
Auto-Immune Hemolytic Anemia	D59.1 - Other autoimmune hemolytic anemias
Bronchiectasis	J47 - Bronchiectasis
Dysmorphic Features	Q02 - Microcephaly; Q18.9 - Congenital Malformation of Face/Neck, Skeletal System; R62.52 - Short Stature; Z36.4 - Intrauterine Growth Restriction; Q82.4 - Ectodermal Dysplasia
Encephalitis	A83 - Mosquito-borne viral encephalitis; A84 - Tick-borne viral encephalitis; A85 - Other viral encephalitis; A86 - Not Elsewhere Classified; G04 - Unspecified Viral Encephalitis, Encephalitis, myelitis and encephalomyelitis
Eosinophilia	D72.1 - Eosinophilia
Failure to Thrive	R62 - Lack of expected normal physiological development in childhood and adults
Fatigue	R53 - Malaise and fatigue
Fibrosis	K74 - Fibrosis and cirrhosis of liver
Granulomatous disease of skin	L92 - Granulomatous disorders of skin and subcutaneous tissue
Herpes Infections	A60 - Anogenital herpes viral [herpes simplex] infections; B00 - Herpes viral [herpes simplex] infections; B02 - Zoster [herpes zoster]; B10 - Other human herpesviruses; B27.0 - Epstein Barr Virus/Mono
Hypocalcemia	E83.51 - Hypocalcemia
Iron Deficiency Anemia	D50.8 - Other iron deficiency anemias
Lymphadenopathy/ Generalized Enlarged Lymph Nodes	R59.9 - Enlarged lymph nodes, Unspc.
Lymphoma	C81 - Hodgkin lymphoma; C82 - Follicular lymphoma; C83 - Non-follicular lymphoma; C84 - Mature T/NK-cell lymphomas; C85 - Other specified and unspecified types of non-Hodgkin lymphoma; C86- Other specified types of T/NK-cell lymphoma; C88 - Malignant immunoproliferative diseases and certain other B-cell lymphomas
Lymphopenia	D72.810 - Lymphocytopenia
Meningococcal Disease	(A39.xx)*- Data learned from literature. For reference, relevant ICD10 codes include A39.xx.
Mycobacterial Disease	A31.9 - Mycobacterial infection, unspecified
Neutropenia	D70 - Neutropenia
Opportunistic Infections	A02 - Other salmonella infections; A31 - Infection due to other mycobacteria; B39 - Histoplasmosis; B40 - Blastomycosis; B55 - Leishmaniasis; B59 - Pneumocystis
Organomegaly	R16 - Hepatomegaly and splenomegaly, NEC
Otorrhea	H92.1 - Otorrhea
Pneumonia	J13 - Pneumonia due to Streptococcus pneumoniae; J14 - Pneumonia due to Hemophilus influenzae; J15 - Bacterial pneumonia (not elsewhere classified); J16 - Pneumonia due to other infectious organisms (not elsewhere classified); J17 - Pneumonia in diseases classified elsewhere; J18 - Pneumonia (unspecified organism)
Polyarthritis	M13 - Other arthritis; M00 - Pyogenic arthritis
Recurrent Fever	A68 - Relapsing fevers
Sensorineural hearing loss	H90 - Conductive and sensorineural hearing loss
Sepsis	A40 - Streptococcal Sepsis; A41 - Other Sepsis; O85 - Puerperal Sepsis; P36 - Bacterial Sepsis
Septic Shock	A41.9 - Sepsis (unspecified organism); R65.21 - Severe sepsis with septic shock
Sinusitis	J01 - Acute Sinusitis; J32 - Chronic Sinusitis
Superficial Mycosis	B36.9 - Superficial Mycosis, Unspc.
Systemic Lupus Erythematosus	L93 - Lupus Erythematosus; M32.9 - Systemic Lupus Erythematosus, unspecified
Thrombocytopenia	D59.59 - Other secondary thrombocytopenia; T45.IX5A - Adverse effect of antineoplastic and immunosuppressive drugs (initial encounter)
Warts	B07 - Viral Warts, etc.

Supplemental Table 2: Immunodeficiency ICD10 Diagnoses for the PI Cohort (n = 1762)

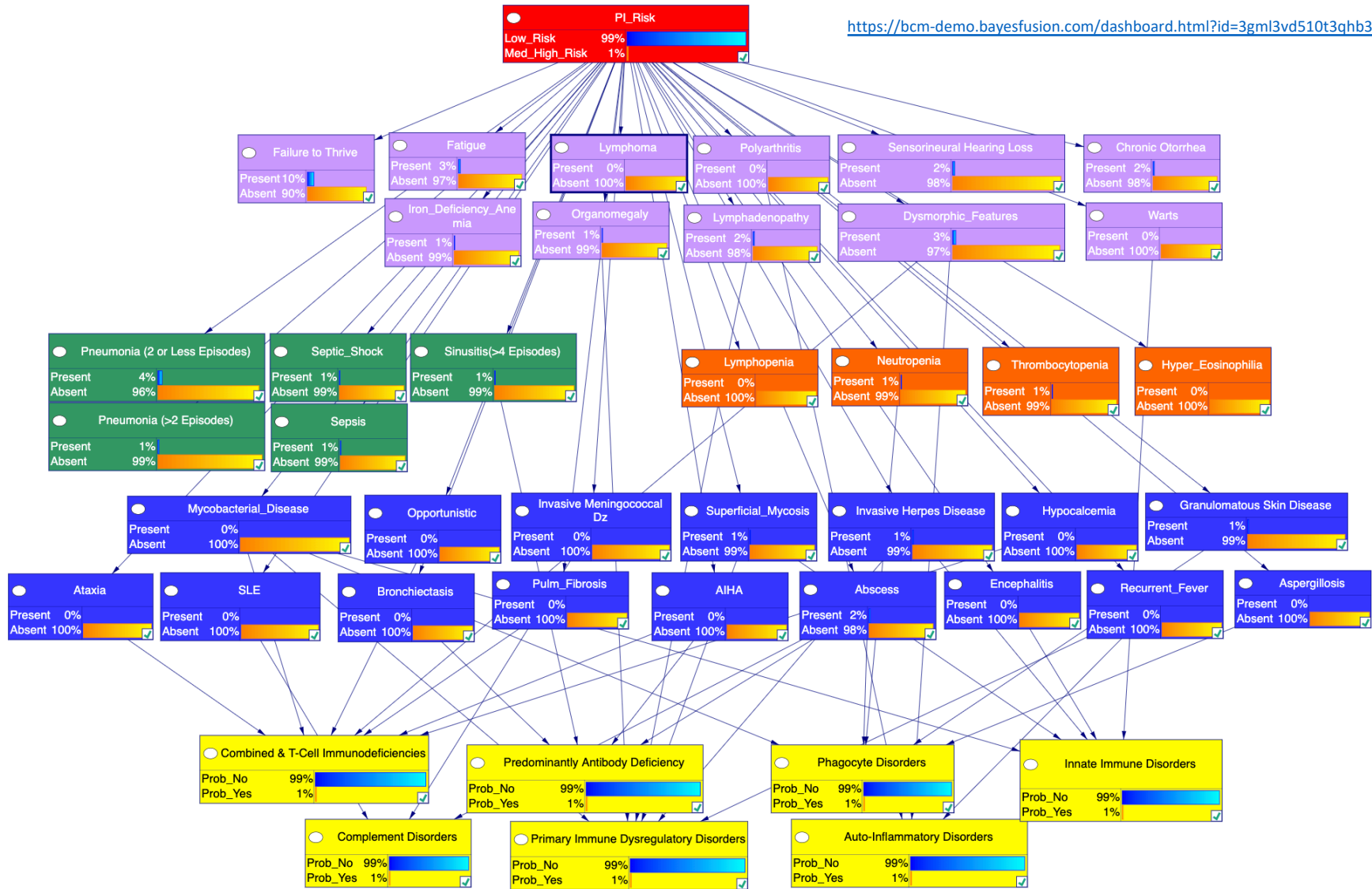
Diagnosis	Count (%)
Functional Disorders of Polymorphonuclear Neutrophils (D71)	34 (1.9%)
Immunodeficiency with Predominantly Antibody Defects (D80)	727 (41.3%)
Combined Immunodeficiencies (D81)	27 (1.5%)
Immunodeficiency Associated with Other Major Defects (D82)	314 (17.8%)
Common Variable Immunodeficiency (D83)	76 (4.3%)
Other Immunodeficiencies (D84)	872 (49.5%)
Other Disorders Involving the Immune Mechanism, Not Elsewhere Classified (D89)	279 (15.8%)

Note: Some patients had ICD10 codes associated with more than one of the diagnosis categories.

Supplemental Fig. Web Interface-Network & Dashboard 1 **A.1** The native BN structure and low-risk probabilities specified are shown. Users can see background probabilities for low/high risk and select nodes here if desired. **A.2** Native dashboard interface. Users can select features along the right sidebar and see risk and top diagnosis prediction displayed on the left panels. **B.1** A case example of network information flow upon entering clinical data for a patient with X-linked agammaglobulinemia (XLA). **B.2** Dashboard output showing the most likely disease category (antibody deficiency) promoted to the top and risk calculation for the XLA patient. **C.1** A case example of network information flow for a patient with chronic granulomatous disease (CGD) and associated findings. **C.2** Dashboard output for the CGD patient displaying the most likely disease category (phagocyte disorder) promoted to the top with associated risk calculation. Note the arrows designating changes from the baseline probabilities as patient characteristics are entered.

A.1

<https://bcm-demo.bayesfusion.com/dashboard.html?id=3gml3vd510t3qhb366xg3uevp>



A.2

<https://bcm-demo.bayesfusion.com/dashboard.html?id=3gml3vd510t3qhb366xg3uevp>

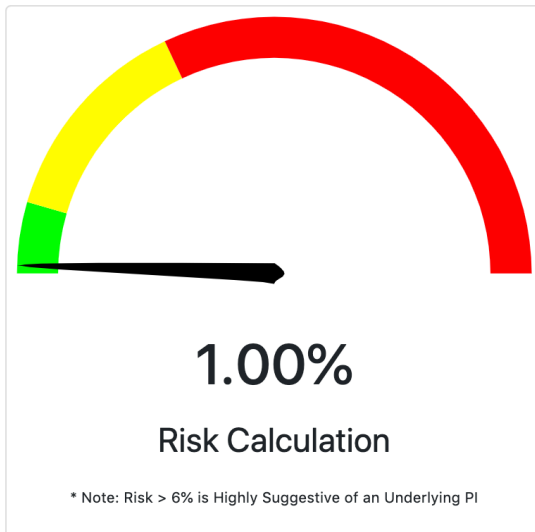


A Probabilistic Tool for Assessing Risk of Primary Immunodeficiency

Network ?



Clinical Guidance: Most Likely Disease Category

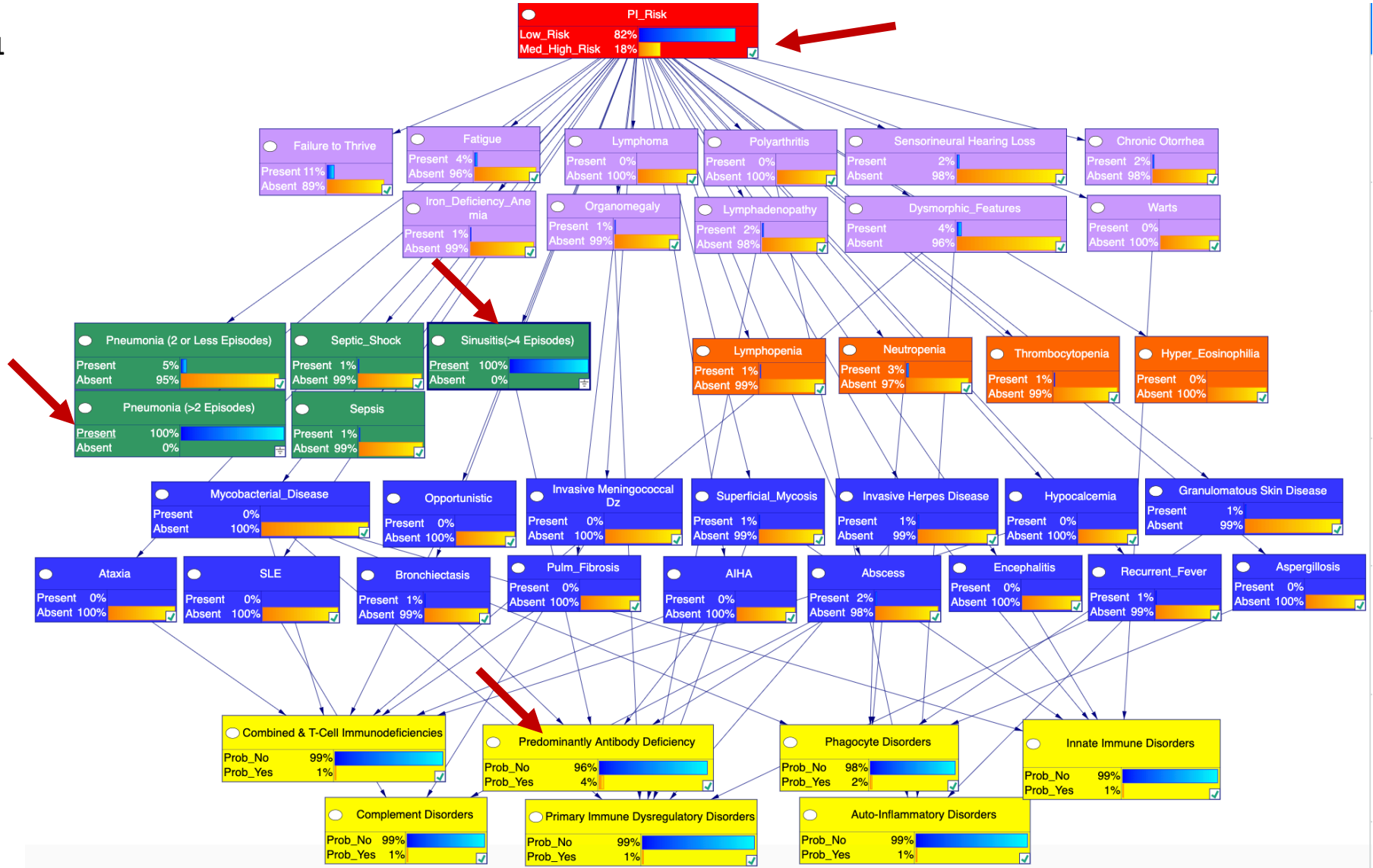


search
Observed
Unobserved
Abscess <ul style="list-style-type: none">• Present• Absent
AIHA <ul style="list-style-type: none">• Present• Absent
Aspergillosis <ul style="list-style-type: none">• Present• Absent
Ataxia <ul style="list-style-type: none">• Present• Absent
Bronchiectasis <ul style="list-style-type: none">• Present• Absent
Chronic Otorrhea <ul style="list-style-type: none">• Present• Absent
Dysmorphic_Features <ul style="list-style-type: none">• Present• Absent

Rider, Nicholas L. 2020

Powered by BayesBox

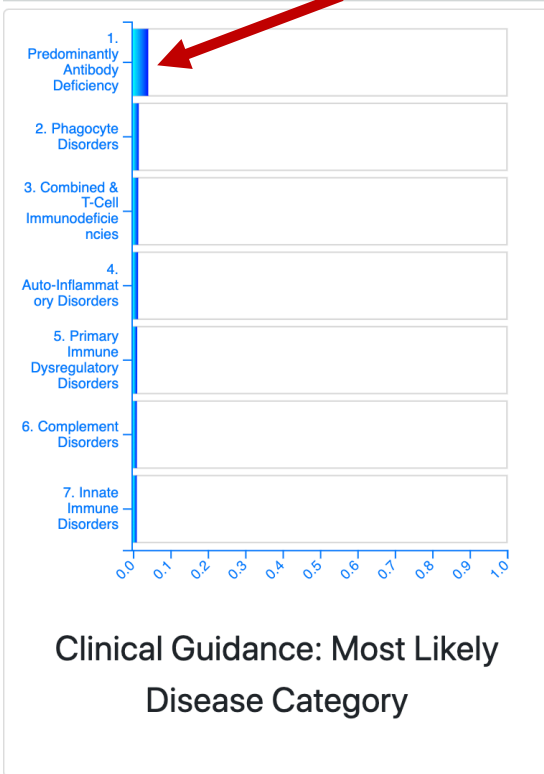
B.1



B.2



A Probabilistic Tool for Assessing Risk of Primary Immunodeficiency



Network ?

search

Observed

Pneumonia (>2 Episodes)
(Present)

- Present
- Absent

Sinusitis(>4 Episodes)
(Present)

- Present
- Absent

Unobserved

Abscess

- Present
- Absent

AIHA

- Present
- Absent

Aspergillosis

- Present
- Absent

Ataxia

- Present
- Absent

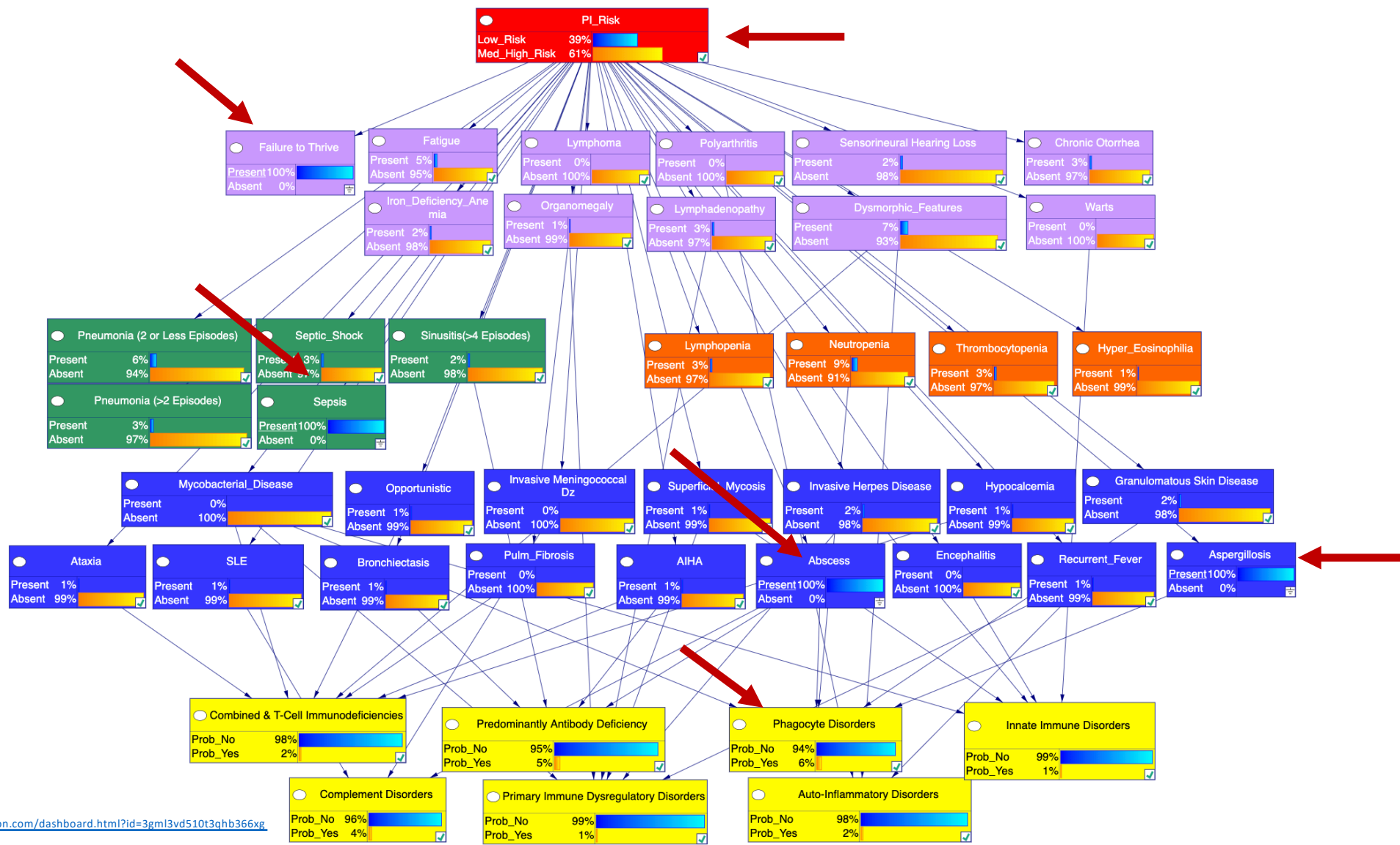
Bronchiectasis

Rider, Nicholas L. 2020

Powered by BayesBox

<https://bcm-demo.bayesfusion.com/dashboard.html?id=3gml3vd510t3qhb366xg3uevp>

C.1



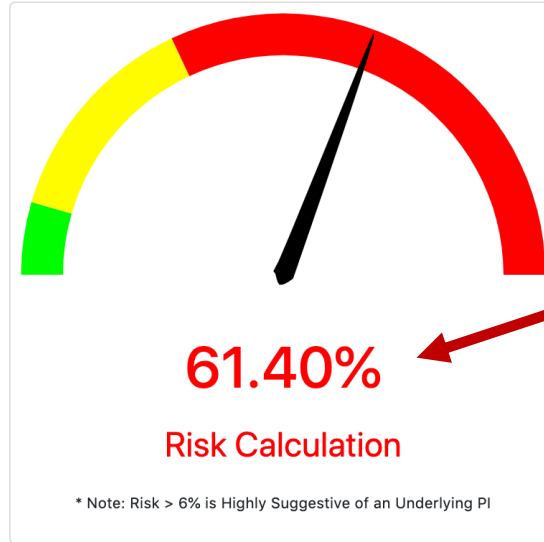
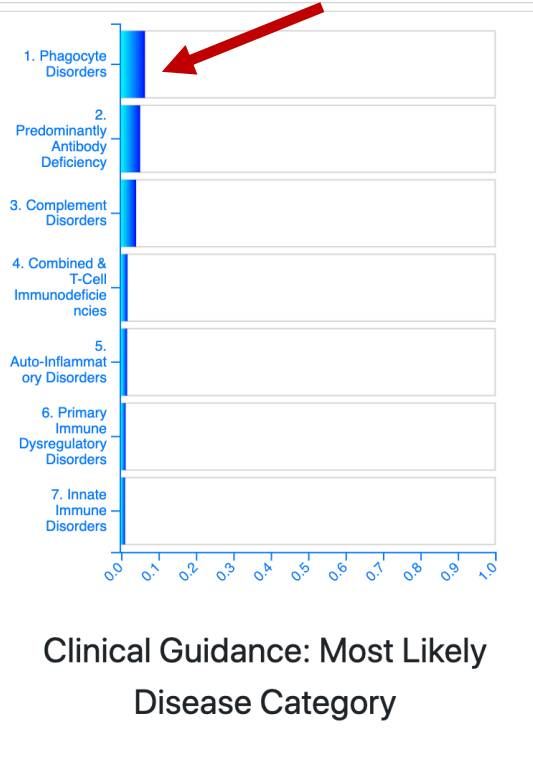
<https://bcm-demo.bayesfusion.com/dashboard.html?id=3gml3vd510t3qhb366xg3uevp>

C.2



A Probabilistic Tool for Assessing Risk of Primary Immunodeficiency

Network ?



search
Observed
<input type="checkbox"/> Abscess (Present) <ul style="list-style-type: none">PresentAbsent
<input type="checkbox"/> Aspergillosis (Present) <ul style="list-style-type: none">PresentAbsent
<input type="checkbox"/> Failure to Thrive (Present) <ul style="list-style-type: none">PresentAbsent
<input type="checkbox"/> Septic_Shock (Present) <ul style="list-style-type: none">PresentAbsent
Unobserved
AIHA <ul style="list-style-type: none">PresentAbsent
Ataxia <ul style="list-style-type: none">PresentAbsent
Bronchiectasis <ul style="list-style-type: none">PresentAbsent

Rider, Nicholas L. 2020

Powered by BayesBox

<https://bcm-demo.bayesfusion.com/dashboard.html?id=3gml3vd510t3qhb366xg3uevp>